RESEARCH PAPER

Cancer Biology & Therapy 14:3, 271–277; March 2013; © 2013 Landes Bioscience

Identification of the optimal therapeutic antibody for fluorescent imaging of cutaneous squamous cell carcinoma

Kristine E. Day,[1] Lauren N. Beck,[1] C. Hope Heath,[1] Conway C. Huang,[2] Kurt R. Zinn[3] and Eben L. Rosenthal[1,*]

[1]Department of Surgery; University of Alabama at Birmingham; Birmingham, AL USA; [2]Department of Dermatology; University of Alabama at Birmingham; Birmingham, AL USA; [3]Department of Radiology; University of Alabama at Birmingham; Birmingham, AL USA

Keywords: optical imaging, cancer, surgery, cutaneous squamous cell carcinoma, antibody, animal model, fluorescence

Abbreviations: cSCC, cutaneous squamous cell carcinoma; NIR, near-infrared; TBR, tumor-to-background; EGFR, epidermal growth factor receptor; VEGF, vascular endothelial growth factor; IL-6R, interleukin 6 receptor; STSG, split-thickness skin graft

Intraoperative, real-time fluorescence imaging may significantly improve tumor visualization and resection and postoperatively, in pathological assessment. To this end, we sought to determine the optimal FDA approved therapeutic monoclonal antibody for optical imaging of human cutaneous squamous cell carcinoma (cSCC). A near-infrared (NIR) fluorescent probe (IRDye800) was covalently linked to bevacizumab, panitumumab or tocilizumab and injected systemically into immunodeficient mice bearing either cutaneous tumor cell lines (SCC13) or cutaneous human tumor explants. Tumors were then imaged and resected under fluorescent guidance with the SPY, an FDA-approved intraoperative imaging system, and the Pearl Impulse small animal imaging system. All fluorescently labeled antibodies delineated normal tissue from tumor in SCC13 xenografts based on tumor-to-background (TBR) ratios. The conjugated antibodies produced TBRs of 1.2–2 using SPY and 1.6–3.6 using Pearl; in comparison, isotype control antibody IgG-IRDye produced TBRs of 1.0 (SPY) and 0.98 (Pearl). Comparison between antibodies revealed them to be roughly equivalent for imaging purposes with both the SPY and Pearl ($p = 0.89$ SPY, $p = 0.99$ Pearl; one way ANOVA). Human tumor explants were also imaged and tumor detection was highest with panitumumab-IRDye800 when using the SPY (TBR 3.0) and Pearl (TBR 4.0). These data suggest that FDA approved antibodies may be clinically used for intraoperative detection of cSCC.

Introduction

Non-melanoma skin cancer is the most common cancer in the United States and its incidence continues to rise worldwide.[1] Cutaneous squamous cell carcinoma (cSCC) is the second most common subtype of nonmelanoma skin cancer, accounting for 15–39% of all skin malignancies. Unlike almost all cases of basal cell carcinoma, squamous cell carcinoma has a substantial risk of metastasis (1.9–47%)[2,3] and recurrence (5.7–8.1%). Given this potential to behave aggressively, complete excision of the primary tumor is extremely important in reducing morbidity and mortality. Surgical excision, by both conventional methods and Mohs surgery, remains the primary treatment choice for cSCC although low risk lesions may be treated with electrodessication and curettage or cryosurgery.[4] High risk lesions including large lesions or recurrent lesions would benefit from methods to confirm negative margins.

Unfortunately, cSCC arising on the head and neck is most commonly associated with incomplete excision and has higher rates of recurrence and metastasis as compared with cSCC on other parts of the body.[2,4,5] Previous studies have demonstrated primary incomplete excision rates of 6.3–15.9%.[2,6] In those undergoing re-excision of previously incompletely excised lesions, the incomplete excision rates ranged from 28.6–60%.[2,7] In order to attain complete resection with conservative margins, Mohs surgery is most often employed because it has the ability to spare tissue while achieving margin control as evidenced by low five-year recurrence rates.[8,9] However, intraoperative histological sectioning with Mohs surgery is still a costly, time-consuming process and cannot be effectively used for large tumors. It is possible that a real-time imaging modality to visualize cutaneous cancer may improve efficiency and accuracy in cSCC removal.

The development of real-time imaging modalities has focused on the exploitation of the near-infrared (NIR) region (700–900 nm), as it has previously been described to have the optimal characteristics needed for sufficient distinction of tumor from normal tissue.[10] Fluorophores emitting light in the 800-nm region generate better tumor-to-background ratios (TBR) because of increased depth penetration and lower nonspecific fluorescence.[10] The identification of the best targeting strategy to detect cancer by NIR fluorescence, however, has proven more challenging. Many techniques have been proposed, but initial steps with FDA

*Correspondence to: Eben L. Rosenthal; Email: oto@uab.edu
Submitted: 10/04/12; Revised: 11/21/12; Accepted: 12/15/12
http://dx.doi.org/10.4161/cbt.23300

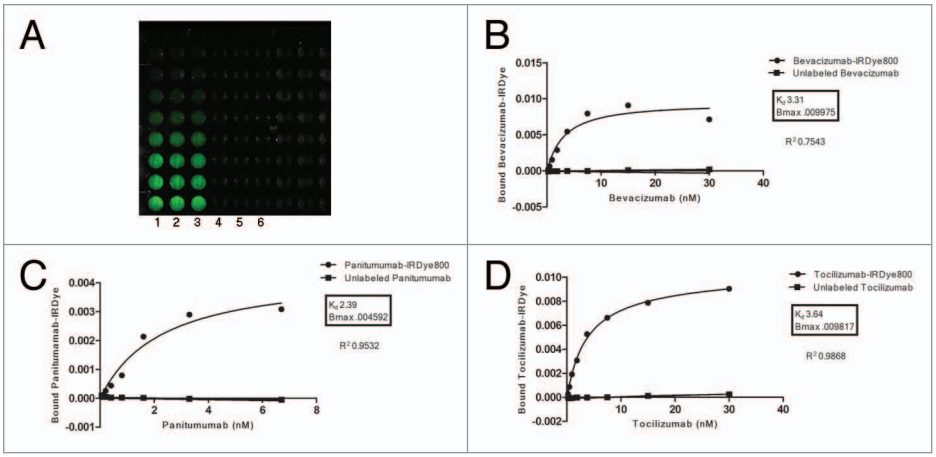

Figure 1. Antigen specificity is retained after conjugation to IRDye800. Three 96-well black plates (bevacizumab shown) were coated in lanes 1–6 with recombinant VEGF, EGFR and IL-6R. Lanes 1–3 were incubated for 1 h with varying concentrations of labeled antibody. For control purposes, wells 4–6 were first blocked with purified, unlabeled antibody and then incubated with the same concentrations of labeled antibody (**A**). The wells were imaged and well intensities quantified with the Pearl impulse imager. Nonlinear regression curves depicting preservation of antigen specificity after IRDye800 labeling were generated using GraphPad Software (**B–D**).

approved antibodies have shown great promise and perhaps represent the best avenue for clinical translation.[11,12] Because cutaneous squamous cell carcinomas are known to express EGFR,[13] VEGF,[14,15] and IL-6R,[16,17] we selected antibodies targeting these ligands for evaluation. These included panitumumab, bevacizumab and tocilizumab, of which, bevacizumab and panitumumab have demonstrated encouraging results in pre-clinical animal models.[18-21]

The purpose of the current study was to demonstrate the visualization of cSCC with both macroscopic and microscopic optical imaging modalities when using antibody targeted fluorescence. We assessed the currently FDA approved antibodies bevacizumab (Avastin), panitumumab (Vectibix) and tocilizumab (Actemra) with the SPY intraoperative imaging hardware and Pearl small animal imager. Our secondary aim was to identify the antibody most suitable for optical imaging with the aforementioned devices.

Results

We first performed a binding affinity test to see if the labeling reaction with the IRDye800 affected the binding affinities of the antibody (**Fig. 1**). We determined that bevacizumab (targeting VEGF), panitumumab (targeting EGFR) and tocilizumab (targeting IL-6R) retained antigen specificity after fluorescent labeling with IRDye800 in vitro.

In order to evaluate in vivo specificity of the antibodies, we then compared the uptake of the three fluorescently labeled antibodies to the uptake of the nonspecific IgG-IRDye800 in mice with SCC13 flank tumors. Because the SPY can be used in the intraoperative setting, tumor fluorescence was initially evaluated with the SPY and compared with the tumor fluorescence obtained with the Pearl, which is the gold standard small animal imaging system designed to detect IRDye800 (**Fig. 2**). TBRs were calculated according to materials and methods. As shown in **Table 1**, all three fluorescently-labeled antigen specific antibodies produced stronger signals as compared with IgG-IRDye800 for both the SPY and Pearl. **Table 1** also shows the p values acquired when comparing each antibody to IgG within each imaging modality. Bevacizumab and panitumumab reached statistical significance ($p = 0.03$ and 0.05) with Pearl when compared with IgG isotype control, while all other values approached statistical significance.

Resection was then accomplished using the SPY system to guide resection of the SCC13 flank tumors (n = 9, average diameter: 7.2 mm, range: 5.1–10.6 mm; average weight: 74.0 mg, range: 23.7–120.4 mg) in real-time until no grossly or fluorescently visible disease remained (figure not shown). When comparing the antibodies against each other using TBR values and a one way ANOVA statistical analysis, we found no difference with either imaging modality (SPY $p = 0.89$ and Pearl $p = 0.99$). Thus, with both imaging modalities, all three antibodies achieved appreciable TBRs indicating that the tumor is clearly differentiated from normal tissue. Conversely, the nonspecific IgG-IRDye800 produced TBRs of 1.0 (SPY) and 0.98 (Pearl), demonstrating equivalent fluorescence intensities between tumor tissue and healthy background tissue and lack of differentiation needed for surgical resection. Because cross reactivity of murine antigens is expected to be low for antibodies designed to target human tissues, the background levels expected in human epithelium is unknown. Therefore, we then evaluated the uptake of each antibody-dye bioconjugate in a tumor vs. human split thickness skin graft (STSG) to establish the expected background fluorescence in humans. The uptake of panitumumab-IRDye800 was evaluated in this way in one of our previous publications.[21] Thus, bevacizumab-IRDye800 and tocilizumab-IRDye800 were assessed in this study with STSGs. Greater fluorescence was confirmed in the tumors vs. the STSGs in all three antibodies (data not shown). The antibody-dye bioconjugates, therefore, were expected to attain TBRs high enough to guide resection.

Optical imaging of a human tumor explant model. To translate the application of optical imaging to human tumors, we transplanted human tumor grafts from a patient with cSCC into the flanks of nude mice (n = 3). We systemically injected each mouse with bevacizumab-IRDye800, panitumumab-IRDye800 or tocilizumab-IRDye800. Tumor fluorescence was assessed with both the SPY and Pearl prior to resection. As shown in **Figure 3A**, all three fluorescently labeled antibodies produced TBRs higher than healthy tissue. When using the SPY, panitumumab-IRDye800 produced the highest TBR (3.0), followed by tocilizumab-IRDye800 (2.5) and bevacizumab-IRDye800 (2.1). When using the Pearl, however, panitumumab-IRDye800

and tocilizumab-IRDye had nearly equivalent TBRs (4.0 vs. 3.9), followed by bevacizumab-IRDye800 (2.8). Bevacizumab, panitumumab and tocilizumab were all shown to be adequate antibodies for imaging human cutaneous SCC tumors (**Fig. 3B**).

As described above, the SPY system was used to guide resection. Areas of residual disease that were not appreciated by palpation or gross visual inspection could be detected by fluorescence on the SPY and correlated with fluorescence detected by the Pearl. The primary tumor, residual areas of positive fluorescence and margins were again sent for histological analysis. Tumor pathology was confirmed by histology and correlated with fluorescence detected by the Odyssey scanner (**Fig. 4**).

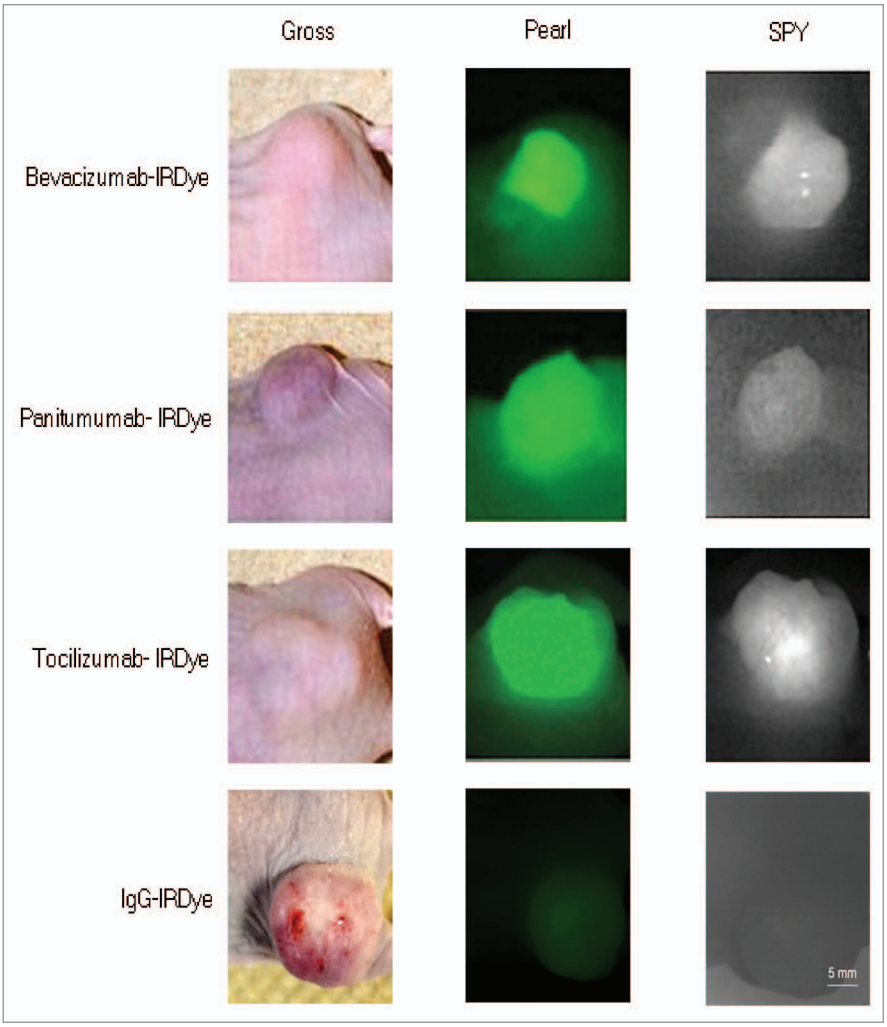

Figure 2. The antibody-dye conjugates were assessed against IgG-IRDye800. Tumor uptake and detection of the antibody-dye conjugates compared with the IgG-IRDye800 control is shown in mice with SCC13 tumors using the SPY and Pearl systems. The conjugated antibodies produced TBRs of 1.2–2 using SPY and 1.6–3.6 using Pearl; in comparison, isotype control antibody IgG-IRDye produced TBRs of 1.0 (SPY) and 0.98 (Pearl). However, comparison between antibodies revealed them to be roughly equivalent for imaging purposes with both the SPY and Pearl ($p = 0.89$ SPY, $p = 0.99$ Pearl; one way ANOVA).

Discussion

There has been significant attention to the development of cancer-specific optical contrast agents which could be used in the operating room to guide real-time surgical evaluation of surgical margins or involved regional lymph nodes.[11] We assessed FDA approved antibodies for cancer specific targeting since the barrier to clinical translation will be lower compared with unique agents. Because a targeted therapeutic agent has not been developed for the targeting of cutaneous squamous cell carcinoma, we present data comparing several antibodies compared with one another in this tumor type. Compared with isotype control or normal human epithelium, the tumor to background ratio was higher when the targeted antibody was assessed. Although all three antibodies demonstrated good contrast and therefore good tumor-to-background ratios, none were significantly better than the other.

This is the first study to evaluate the potential benefit of optical imaging in cutaneous cancer which is amendable to optical imaging because of the surface nature of this disease. Furthermore, we demonstrate that conventional operating room equipment can be used to image antibody labeled with IRDye800. We demonstrate that each antibody has similar tumor-to-background ratios, although the Pearl imaging system is clearly superior to the SPY imaging system. In the last decade, the field of optical imaging has shown incredible growth. Almost half of all articles on optical imaging of cancer have been published in the past 5 y.[22] Multiple strategies have been investigated including quantum dot nanoparticles as a targeting ligand,[23] bioluminescent imaging (BLI) using luciferase vector,[24] and cleavable NIR probes that are activated by proteases secreted by tumors.[25,26] Quantum dots, however, exhibit serious toxicity concerns and BLI is not feasible in humans as it requires genetic alterations of the cancer cells. Agents targeting proteases are also unsuitable as cathepsins and matrix metalloproteinases are not only produced by cancer cells, but also macrophages and neutrophils.[27] Antibodies thus present themselves as the most promising imaging agent because of their established pharmacokinetics and safety in humans. These therapeutic agents have already successfully undergone phase III trials and greatly reduce any translational risks.

This is the first study using tocilizumab as a potential tumor targeted imaging agent. Though its pattern of expression has not been specifically investigated in cSCC, IL-6R is known to be expressed in head and neck SCC.[16,17] However, IL-6 is a multifunctional cytokine that regulates immune responses and acute phase reactions,[28] and therefore its receptor may not prove to be a specific tumor marker. Because an immunosuppressed

Table 1. Antibody comparison to nonspecific IgG in SCC13 flank tumors

SPY	Avg antibody TBR	IgG TBR	p values‡	95% CI
Bevacizumab vs IgG	1.49 (n = 3)	1.02†	0.07	-0.07458–1.017
Panitumumab vs IgG	1.62 (n = 3)		0.11	-0.3514–1.551
Tocilizumab vs IgG	1.50 (n = 3)		0.20	-0.6069–1.566
PEARL				
Bevacizumab vs IgG	2.70 (n = 3)	0.98†	0.03*	0.3055–3.138
Panitumumab vs IgG	2.66 (n = 3)		0.05*	-0.08456–3.447
Tocilizumab vs IgG	2.75 (n = 3)		0.10	-0.8020–4.337

Bevacizumab and panitumumab achieved p values < 0.05 when compared with nonspecific IgG when using the Pearl. All others trended toward statistical significance. †Reflects a single set of IgG experiments that was performed. ‡Paired t-tests were calculated using GraphPad Prism software.

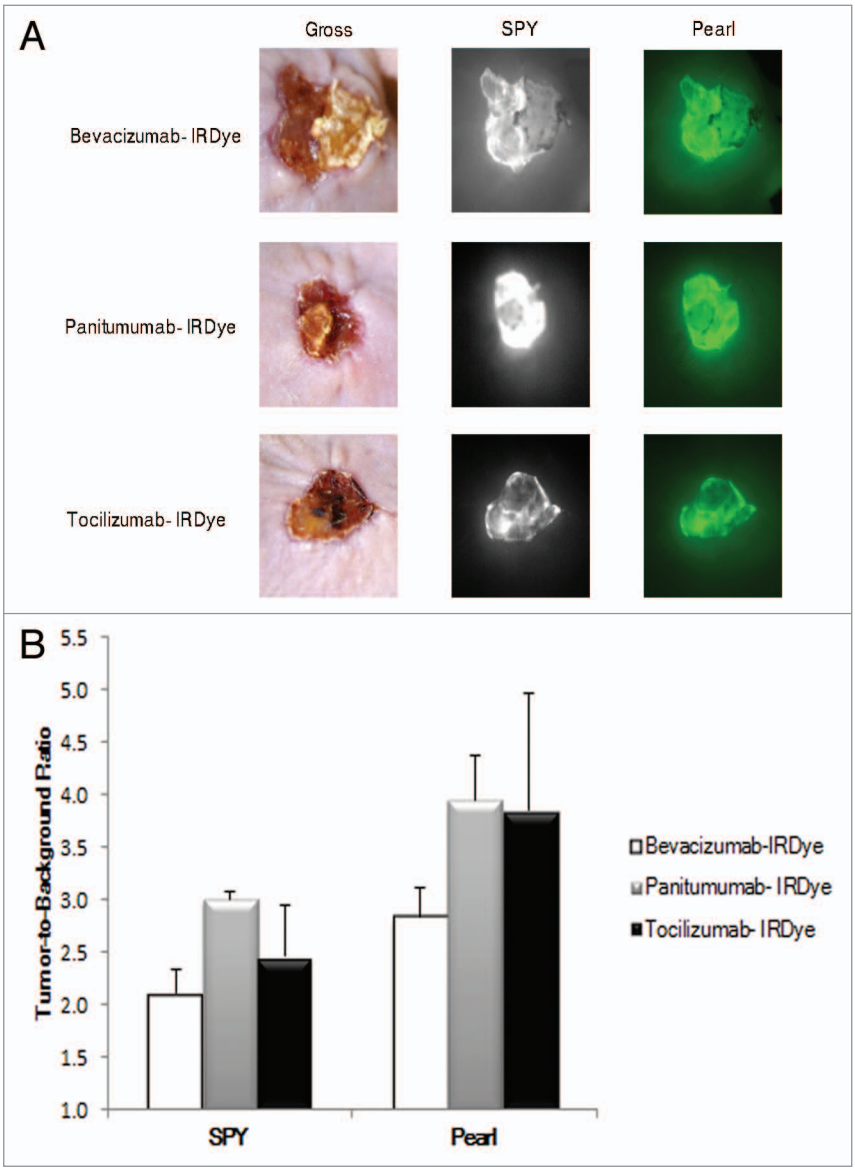

Figure 3. The antibody-dye conjugates were evaluated in human tumor explants. Imaging with the SPY and Pearl in mice with human cSCC tumor explants shows good tumor uptake and detection (**A**). Panitumumab-IRDye800 produced a higher TBR with the SPY and Pearl (**B**).

model has limited inflammatory cells, the background of IL-6R positive cells is not likely to be in the stromal tissues of the murine model. Tumor specific antigens such as EGFR and VEGF are likely to be more tumor-specific in human tumors. Sweeny et al., has indeed shown EGFR to be expressed in approximately 56% of cSCC primary tumors and 58% of regional metastatic disease.[29] In another study, widespread expression of VEGF was seen in 78% of cSCC cases examined and also demonstrated a statistically significant difference ($p < 0.001$) in expression when compared with normal skin.[30] These antigens, therefore, present a higher likelihood of specificity. In our previous work, panitumumab and bevacizumab have proven effective for tumor targeting purposes in other head and neck cancers. In one study, panitumumab-IRDye800 (targeting EGFR) achieved TBRs of 2.3 (SPY) and 2.9 (Pearl) in oral SCC in preclinical murine models.[21] Bevacizumab conjugated to the Cy 5.5 fluorophore achieved a sensitivity and specificity of 80.9 and 91.7% with resections.[19] A 2007 study has since shown IRDye800CW to have better tissue penetration and produce improved TBRs compared with Cy5.5,[31] leading to our current conjugation and investigation with IRDye800. In addition to head and neck cancer, bevacizumab-IRDye800 has also proved to be effective in other cancers such as ovarian, breast and gastric.[20] In fact, a clinical trial investigating the use of bevacizumab-IRDye800 in breast cancer imaging is currently underway in the Netherlands.[32]

A possible limitation to our study is the imaging equipment used. The SPY imaging system is designated for use with indocyanine green (ICG) in determining blood vessel and graft patency. This makes the translational potential higher, but it should be noted that the range at which ICG can be imaged is 820–840 nm, whereas the range for IRDye800 is somewhat lower at 780–800 nm. The wavelengths are

similar, but this difference may have contributed to our lower TBRs with the SPY. Also, the mouse tumors may not be the best representation of human cSCC. Since the tumors are usually more circumscribed, they do not readily mimic the usual presentation of cSCC as a non-healing ulcer in humans and thus limit exact evaluation of subclinical disease and its resection. Lastly, though a study by Marshall et al. demonstrated no toxic or adverse effects in rats in doses up to 20 mg/kg,[33] IRDye800 is not approved for human use and presents a barrier to clinical translation. At present, ICG is the only NIR fluorophore approved for human use in the US. A major shortcoming of ICG, however, is that it lacks a reactive functional group and therefore, cannot be used to label targeting agents.[33]

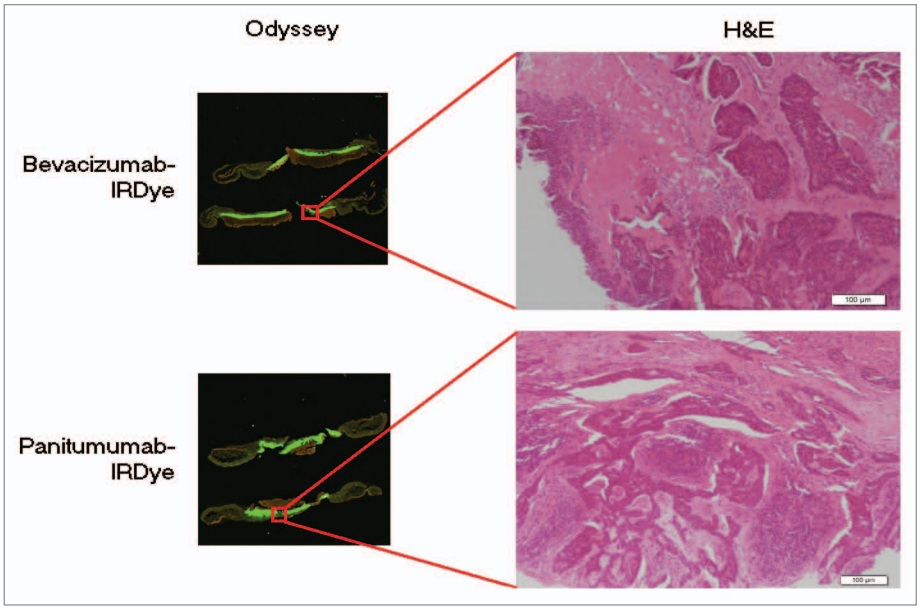

Figure 4. Pathologic and fluorescent microscopic imaging of the cSCC human tumor explants. Tumor cells on H&E correlate with areas of fluorescence using the Odyssey microscopic imager.

Because most cancers are heterogeneous in nature and may exhibit different expression patterns, it may be that combinations of labeled tumor-targeting agents are necessary to completely visualize cancers in the surgical bed. Variations in tumor antigens, both between tumors and within a tumor, could potentially influence fluorescence intensity. These differences make the use of probe "cocktails" an encouraging future direction to undertake.[34] The technique of dual wavelength tumor targeting has been explored in hypopharyngeal cancer and breast cancer models.[34,35] Another promising approach lies in dual-labeling tumor targeting agents to radioactive substances in order to increase the accuracy of pre and post-operative radiographic scans. Nguyen et al. successfully used MRI and fluorescence to decrease residual cancer and improve survival in a preclinical murine model.[36] Perhaps the most important subject for future research though, is detection thresholds of fluorescent agents. The minimal detectable amount of cells has yet to be determined and has direct implications for clinical translatability.[34]

In conclusion, our data show antibodies to be an effective tumor targeting strategy in NIR real-time fluorescent imaging of cutaneous squamous cell carcinoma. This strategy offers the advantage of utilizing FDA approved agents and warrants continued clinical investigations.

Materials and Methods

Cell lines and tissue culture. A human tumor explant and one cSCC cell line (SCC13) were used. The human tumor explants were harvested from a patient with cSCC receiving surgical treatment at The University of Alabama at Birmingham. The SCC13 cell line was kindly received from the laboratory of Santosh Katiyar, PhD (University of Alabama at Birmingham). The cell line was grown and maintained in Dulbecco's modified Eagle's medium (DMEM) containing 10% fetal bovine serum (FBS) and supplemented with 1% penicillin, streptomycin and amphotericin B. It was incubated at 37°C in 5% CO_2.

Reagents. Bevacizumab (Avastin, Genentech; 149 kDa), panitumumab (Vectibix, Amgen; 147 kDa) and tocilizumab (Actemra, Genentech; 148 kDa) were the antibodies used. Protein A purified IgG antibody (Innovative; Ir-Hu-Gf, 30010BM; 146kDa) was used as a control antibody.

NIR fluorescence agents. IRDye800CW (IRDye800CW-*N*-hydroxysuccinimide ester, LI-COR Biosciences) was the fluorescent probe. It has a NIR absorption and emission peak of 778/794 nm. When conjugated to an antibody the absorbance and emission maximums decrease slightly (774/789 nm).[37] Bevacizumab, panitumumab, tocilizumab and IgG were labeled according to the manufacturers' protocol. Briefly, the antibodies were incubated with the IRDye800CW for 2 h and the unconjugated dye was removed by desalting columns (Pierce, Zeba, 89891).

Antigen detection assay. Three different assays were performed for each of the three antibodies. Six lanes of a 96-well black plate were coated with recombinant EGFR (rEGFR/ErbB1; 400 ng/well/100μL; Fc Chimera, 344-ER), IL-6R (rIL-6Rα; 400 ng/well/100μL; 227-SR/CF) or VEGF (rVEGF; 100 ng/well/100 μL; 293-VE/CF) overnight at 4°C. The wells were blocked for 1 h at room temperature with 1% bovine serum albumin (BSA). Wells were then washed with phosphate-buffered saline (PBS) three times. For control purposes, purified antibody was added to three lanes of coated wells and allowed to block for 1 h. Serial dilutions of labeled antibody (0.234375–30 nM for bevacizumab and tocilizumab; 0.05–6.7 nM for pantiumumab) were then added to all coated wells and incubated for 1 h. Uncoated wells on the same plate were also maintained for background control. After incubation, the wells were washed with PBS and imaged using the Pearl (Li-Cor Biosciences). Well

intensities were quantified using the Pearl Impulse software, version 2.0.

Animal models. Nude (nu/nu) mice (Charles River Laboratories), aged 4–6 weeks, were obtained and housed in accordance with the Institutional Animal Care and Use Committee (IACUC) guidelines. All experiments were conducted and the mice euthanized according to IACUC guidelines.

For the SCC13 flank model, mice (n = 10) received subcutaneous injections of SCC13 cells (2×10^6) suspended in media (200 μL). Tumor size was monitored weekly until they reached 25 mm^2. The mice were then systemically injected with one of the three fluorescently labeled antibodies or IgG (50–100 μg). For the human tumor explant model, the skin from the back of nude mice was excised and the tumor explants sutured in place with absorbable suture. These were monitored for several days prior to injection to ensure the grafts survived the explantation process.

Fluorescence imaging and measurement. The SPY imaging system captures fluorescent light using a charged couple device video camera at 30 frames per second and displays it on a computer monitor.[38] This system was used to guide tumor resections at 48–96 h post injection of the fluorescently-labeled antibodies. Since the Pearl Impulse small animal imaging system (LI-COR Biosciences) is specifically designed to image IRDye800, the animals were also imaged by this device in order to verify and co-localize the fluorescence seen by SPY. Following tumor and margin resections, the excised tissues were placed in cassettes and imaged with both the SPY and the Pearl. In vivo fluorescence detected with the SPY machine was quantified using ImageJ software.[39] Fluorescence intensity was measured by selecting several regions of interest (ROI) within the tumor and calculating the mean value. Subsequently, a tumor-to-background ratio (TBR) was calculated based on the fluorescence intensity from a sample of normal tissue adjacent to the tumor border.

For the human tumor explant model, fluorescent microscopy of histologic sections was performed using the Odyssey scanner (LI-COR Biosciences). Co-localization of the fluorescent signal with tumor was performed by overlaying the Odyssey-acquired fluorescent image with the microscopic H&E image.

Statistical analysis. To compare the TBRs for each antibody in the SCC13 tumor model, a one-way ANOVA with Tukey's post-test was performed using GraphPad Prism version 5.04 for Windows, GraphPad Software, www.graphpad.com. Error bars represent the standard deviation. TBRs of each antibody-dye bioconjugate were also compared with the control IgG-dye conjugate using paired t-tests. Statistical significance was considered $p < 0.05$.

Disclosure of Potential Conflicts of Interest

The authors have no conflicts of interest.

Acknowledgments

Work was supported by grant from NIDCR (R21DE019232) and equipment donated by Novadaq. IRDye800 was supplied by LI-COR Biosciences.

References

1. Lomas A, Leonardi-Bee J, Bath-Hextall F. A systematic review of worldwide incidence of nonmelanoma skin cancer. Br J Dermatol 2012; 166:1069-80; PMID:22251204; http://dx.doi.org/10.1111/j.1365-2133.2012.10830.x.
2. Tan PY, Ek E, Su S, Giorlando F, Dieu T. Incomplete excision of squamous cell carcinoma of the skin: a prospective observational study. Plast Reconstr Surg 2007; 120:910-6; PMID:17805118; http://dx.doi.org/10.1097/01.prs.0000277655.89728.9f.
3. Brougham ND, Dennett ER, Cameron R, Tan ST. The incidence of metastasis from cutaneous squamous cell carcinoma and the impact of its risk factors. J Surg Oncol 2012; 106:811-5; PMID:22592943; http://dx.doi.org/10.1002/jso.23155.
4. Alam M, Ratner D. Cutaneous squamous-cell carcinoma. N Engl J Med 2001; 344:975-83; PMID:11274625; http://dx.doi.org/10.1056/NEJM200103293441306.
5. Talbot S, Hitchcock B. Incomplete primary excision of cutaneous basal and squamous cell carcinomas in the Bay of Plenty. N Z Med J 2004; 117:U848; PMID:15107870.
6. Ang P, Tan AW, Goh CL. Comparison of completely versus incompletely excised cutaneous squamous cell carcinomas. Ann Acad Med Singapore 2004; 33:68-70; PMID:15008566.
7. Bovill ES, Cullen KW, Barrett W, Banwell PE. Clinical and histological findings in re-excision of incompletely excised cutaneous squamous cell carcinoma. J Plast Reconstr Aesthet Surg 2009; 62:457-61; PMID:18218349; http://dx.doi.org/10.1016/j.bjps.2007.11.041.
8. Pugliano-Mauro M, Goldman G. Mohs surgery is effective for high-risk cutaneous squamous cell carcinoma. Dermatol Surg 2010; 36:1544-53; PMID:21053415; http://dx.doi.org/10.1111/j.1524-4725.2010.01576.x.
9. Leibovitch I, Huilgol SC, Selva D, Hill D, Richards S, Paver R. Cutaneous squamous cell carcinoma treated with Mohs micrographic surgery in Australia I. Experience over 10 years. J Am Acad Dermatol 2005; 53:253-60; PMID:16021120; http://dx.doi.org/10.1016/j.jaad.2005.02.059.
10. Keereweer S, Kerrebijn JD, Mol IM, Mieog JS, Van Driel PB, Baatenburg de Jong RJ, et al. Optical imaging of oral squamous cell carcinoma and cervical lymph node metastasis. Head Neck 2012; 34:1002-8; PMID:21987435; http://dx.doi.org/10.1002/hed.21861.
11. Keereweer S, Kerrebijn JD, van Driel PB, Xie B, Kaijzel EL, Snoeks TJ, et al. Optical image-guided surgery--where do we stand? Mol Imaging Biol 2011; 13:199-207; PMID:20617389; http://dx.doi.org/10.1007/s11307-010-0373-2.
12. Scheuer W, van Dam GM, Dobosz M, Schwaiger M, Ntziachristos V. Drug-based optical agents: infiltrating clinics at lower risk. Sci Transl Med 2012; 4:34ps11; PMID:22593172; http://dx.doi.org/10.1126/scitranslmed.3003572.
13. Bonner JA, De Los Santos J, Waksal HW, Needle MN, Trummel HQ, Raisch KP. Epidermal growth factor receptor as a therapeutic target in head and neck cancer. Semin Radiat Oncol 2002; 12(Suppl 2):11-20; PMID:12174340; http://dx.doi.org/10.1053/srao.2002.34864.
14. Kyzas PA, Stefanou D, Batistatou A, Agnantis NJ. Prognostic significance of VEGF immunohistochemical expression and tumor angiogenesis in head and neck squamous cell carcinoma. J Cancer Res Clin Oncol 2005; 131:624-30; PMID:16044346; http://dx.doi.org/10.1007/s00432-005-0003-6.
15. Thomas GR, Nadiminti H, Regalado J. Molecular predictors of clinical outcome in patients with head and neck squamous cell carcinoma. Int J Exp Pathol 2005; 86:347-63; PMID:16309541; http://dx.doi.org/10.1111/j.0959-9673.2005.00447.x.
16. Shinriki S, Jono H, Ota K, Ueda M, Kudo M, Ota T, et al. Humanized anti-interleukin-6 receptor antibody suppresses tumor angiogenesis and in vivo growth of human oral squamous cell carcinoma. Clin Cancer Res 2009; 15:5426-34; PMID:19706815; http://dx.doi.org/10.1158/1078-0432.CCR-09-0287.
17. Wang YF, Chang SY, Tai SK, Li WY, Wang LS. Clinical significance of interleukin-6 and interleukin-6 receptor expressions in oral squamous cell carcinoma. Head Neck 2002; 24:850-8; PMID:12211049; http://dx.doi.org/10.1002/hed.10145.
18. Gleysteen JP, Duncan RD, Magnuson JS, Skipper JB, Zinn K, Rosenthal EL. Fluorescently labeled cetuximab to evaluate head and neck cancer response to treatment. Cancer Biol Ther 2007; 6:1181-5; PMID:17637562.
19. Withrow KP, Newman JR, Skipper JB, Gleysteen JP, Magnuson JS, Zinn K, et al. Assessment of bevacizumab conjugated to Cy5.5 for detection of head and neck cancer xenografts. Technol Cancer Res Treat 2008; 7:61-6; PMID:18198926.
20. Terwisscha van Scheltinga AG, van Dam GM, Nagengast WB, Ntziachristos V, Hollema H, Herek JL, et al. Intraoperative near-infrared fluorescence tumor imaging with vascular endothelial growth factor and human epidermal growth factor receptor 2 targeting antibodies. J Nucl Med 2011; 52:1778-85; PMID:21990576; http://dx.doi.org/10.2967/jnumed.111.092833.
21. Heath CH, Deep NL, Sweeny L, Zinn KR, Rosenthal EL. Use of panitumumab-IRDye800 to image microscopic head and neck cancer in an orthotopic surgical model. Ann Surg Oncol 2012; 19:3879-87; PMID:22669455; http://dx.doi.org/10.1245/s10434-012-2435-y.
22. Rosenthal E. ZKR. Optical Imaging of Cancer. New York: Springer, 2009.

23. Mulder WJ, Castermans K, van Beijnum JR, Oude Egbrink MG, Chin PT, Fayad ZA, et al. Molecular imaging of tumor angiogenesis using alphavbeta3-integrin targeted multimodal quantum dots. Angiogenesis 2009; 12:17-24; PMID:19067197; http://dx.doi.org/10.1007/s10456-008-9124-2.
24. Kim JB, Urban K, Cochran E, Lee S, Ang A, Rice B, et al. Non-invasive detection of a small number of bioluminescent cancer cells in vivo. PLoS One 2010; 5:e9364; PMID:20186331; http://dx.doi.org/10.1371/journal.pone.0009364.
25. Wunderbaldinger P, Turetschek K, Bremer C. Near-infrared fluorescence imaging of lymph nodes using a new enzyme sensing activatable macromolecular optical probe. Eur Radiol 2003; 13:2206-11; PMID:12802615; http://dx.doi.org/10.1007/s00330-003-1932-6.
26. Mahmood U, Weissleder R. Near-infrared optical imaging of proteases in cancer. Mol Cancer Ther 2003; 2:489-96; PMID:12748311.
27. Wunder A, Straub RH, Gay S, Funk J, Müller-Ladner U. Molecular imaging: novel tools in visualizing rheumatoid arthritis. Rheumatology (Oxford) 2005; 44:1341-9; PMID:15972356; http://dx.doi.org/10.1093/rheumatology/keh709.
28. Kishimoto T. The biology of interleukin-6. Blood 1989; 74:1-10; PMID:2473791.
29. Sweeny L, Dean NR, Magnuson JS, Carroll WR, Helman EE, Hyde SO, et al. EGFR expression in advanced head and neck cutaneous squamous cell carcinoma. Head Neck 2012; 34:681-6; PMID:21739514; http://dx.doi.org/10.1002/hed.21802.
30. Bowden J, Brennan PA, Umar T, Cronin A. Expression of vascular endothelial growth factor in basal cell carcinoma and cutaneous squamous cell carcinoma of the head and neck. J Cutan Pathol 2002; 29:585-9; PMID:12453295; http://dx.doi.org/10.1034/j.1600-0560.2002.291003.x.
31. Adams KE, Ke S, Kwon S, Liang F, Fan Z, Lu Y, et al. Comparison of visible and near-infrared wavelength-excitable fluorescent dyes for molecular imaging of cancer. J Biomed Opt 2007; 12:024017; PMID:17477732; http://dx.doi.org/10.1117/1.2717137.
32. Dam GMv. VEGF- targeted Fluorescent Tracer Imaging in Breast Cancer. In: ClinicalTrials.gov [Internet]: Bethesda (MD): National Library of Medicine (US). 2000- [cited 2012 Sept 6], 2011.
33. Marshall MV, Draney D, Sevick-Muraca EM, Olive DM. Single-dose intravenous toxicity study of IRDye 800CW in Sprague-Dawley rats. Mol Imaging Biol 2010; 12:583-94; PMID:20376568; http://dx.doi.org/10.1007/s11307-010-0317-x.
34. Keereweer S, Mol IM, Vahrmeijer AL, Van Driel PB, Baatenburg de Jong RJ, Kerrebijn JD, et al. Dual wavelength tumor targeting for detection of hypopharyngeal cancer using near-infrared optical imaging in an animal model. Int J Cancer 2012; 131:1633-40; PMID:22234729; http://dx.doi.org/10.1002/ijc.27430.
35. Xie BW, Mol IM, Keereweer S, van Beek ER, Que I, Snoeks TJ, et al. Dual-wavelength imaging of tumor progression by activatable and targeting near-infrared fluorescent probes in a bioluminescent breast cancer model. PLoS One 2012; 7:e31875; PMID:22348134; http://dx.doi.org/10.1371/journal.pone.0031875.
36. Nguyen QT, Olson ES, Aguilera TA, Jiang T, Scadeng M, Ellies LG, et al. Surgery with molecular fluorescence imaging using activatable cell-penetrating peptides decreases residual cancer and improves survival. Proc Natl Acad Sci U S A 2010; 107:4317-22; PMID:20160097; http://dx.doi.org/10.1073/pnas.0910261107.
37. Biosciences L-C. IRDye(R) 800 CW protein labeling kit–high MW. Lincoln, NE. Li-Cor Biosciences 2007; 2007:1-9.
38. Reuthebuch O, Häussler A, Genoni M, Tavakoli R, Odavic D, Kadner A, et al. Novadaq SPY: intraoperative quality assessment in off-pump coronary artery bypass grafting. Chest 2004; 125:418-24; PMID:14769718; http://dx.doi.org/10.1378/chest.125.2.418.
39. Schneider CA, Rasband WS, Eliceiri KW. NIH Image to ImageJ: 25 years of image analysis. Nat Methods 2012; 9:671-5; PMID:22930834; http://dx.doi.org/10.1038/nmeth.2089.